
Evaluating the effectiveness of predicting covariates in LSTM Networks for Time Series Forecasting

Gareth Davies

Neural Aspect
garethmd@googlemail.com

Abstract

Autoregressive Recurrent Neural Networks are widely employed in time-series forecasting tasks, demonstrating effectiveness in univariate and certain multivariate scenarios. However, their inherent structure does not readily accommodate the integration of future, time-dependent covariates. A proposed solution, outlined by Salinas et al 2019[1], suggests forecasting both covariates and the target variable in a multivariate framework. In this study, we conducted comprehensive tests on publicly available time-series datasets, artificially introducing highly correlated covariates to future time-step values. Our evaluation aimed to assess the performance of an LSTM network when considering these covariates and compare it against a univariate baseline. As part of this study we introduce a novel approach using seasonal time segments in combination with an RNN architecture, which is both simple and extremely effective over long forecast horizons with comparable performance to many state of the art architectures. Our findings from the results of more than 120 models reveal that under certain conditions jointly training covariates with target variables can improve overall performance of the model, but often there exists a significant performance disparity between multivariate and univariate predictions. Surprisingly, even when provided with covariates informing the network about future target values, multivariate predictions exhibited inferior performance. In essence, compelling the network to predict multiple values can prove detrimental to model performance, even in the presence of informative covariates. These results suggest that LSTM architectures may not be suitable for forecasting tasks where predicting covariates would typically be expected to enhance model accuracy.

1 Introduction

Forecasting future events, is a critical endeavour across various domains, facilitating informed decision-making and resource allocation. These forecasting tasks heavily rely on historical data to make accurate predictions. Given the inherent sequential and time-dependent nature of such data, Recurrent Neural Networks (RNNs) emerge as a natural choice for modelling temporal sequences due to their ability to retain memory across time steps.[2]

However, traditional forecasting methods, particularly autoregression, which relies on using past observations to predict future values, encounter challenges as forecasting horizons extend. As predictions are recursively dependent on preceding values, errors can compound over time, resulting in diminished accuracy.

Furthermore, predicting values solely from prior observations prevents analysis of the underlying features that influence future outcomes. Therefore making it impossible to simulate scenarios or identify corrective action. For example during the Covid pandemic the number of positive tests informed future hospitalisation and mortality rates, or the volume of sales meetings could inform

an organisation of future sales. Clearly the inclusion of these leading indicators would be highly desirable both in terms of improving accuracy and our understanding of the domain.

To address these limitations and enhance prediction accuracy, researchers have explored the incorporation of additional information, known as covariates, into forecasting models. Covariates can provide valuable context and assist the network in making more informed predictions. They can be either static time-independent, which are fixed for an entire time-series, or time-dependent, where provided values can change at each time step. When future time-dependent covariates are known in advance, such as week or month numbers, they can be leveraged to augment autoregressive predictions. Conversely, in scenarios where future covariates are unknown, they must either be estimated beforehand or predicted simultaneously with the target variable, rendering each prediction multivariate.

In this study, we aim to evaluate the efficacy of employing autoregressive multivariate Long Short-Term Memory (LSTM) models compared to traditional univariate models without covariates. We conduct our investigation within the context of well-established time series datasets from the Monash repository [3], a widely recognised benchmark for evaluating forecasting models. Our methodology involves constructing baseline univariate models using an autoregressive LSTM, ensuring their performance aligns with established benchmarks. Subsequently, we augment each dataset by introducing covariates engineered from future time-step values, effectively guiding the network in predicting both the target variable and the associated covariate. We then assess the performance of our models based on predicting target values over a forecast horizon H .

The contributions of this study are: 1. A novel approach to modelling timeseries data with LSTM networks that is extremely effective in a univariate setting and does not require specialised feature engineering. 2. Quantification of the effect cross correlation between covariates and target variables has on the resulting performance of a trained model. 3. An evaluation of how model performance is affected as forecast horizons increase. 4. A simple approach to synthesise covariates from univariate datasets for running experiments in a controlled and repeatable manner.

2 Related Work

The use of covariates in State Space models have been studied notably by Wang[4] and more recently by Puindi and Silba [5]. Wang proposed ESCov a method that extended HoltWinters to utilise informative covariates which were calculated in advance of the main modelling task. Wang observed that the inclusion of covariates could improve the overall accuracy of the model, the degree to which is in part determined by the quality of the predictions of the covariates.

Lai et al. [6] developed LSTNet, which supports multivariate scenarios and which combines a CNN and a GRU to capture both long and short-term dependencies over time, as well as local dependencies between variables.

Salinas et al. [1] proposed DeepAR, an autoregressive LSTM model intended to be used specifically for time-series forecasting. Their approach included time dependent covariates as inputs into each timestep combining them with the outputs of the previous timestep to assist the network.

Salinas et al subsequently extended DeepAR to a multivariate setting with DeepVAR and GPVAR [7], which supported scenarios where datasets of multiple timeseries are forecasted simultaneously through vector autoregression. The objective being to model the dynamics between the target variables in each timeseries. As the dimension of the output vector scales, the multivariate predictions can become very high dimensional, and encounter high computational costs as a result. GPVAR addresses this by modifying the output model with a low rank covariance structure.

More recently, transformer-based models such as Reformer, Informer, Autoformer, and CrossFormer [8, 9, 10, 11] have emerged for multivariate predictions. Notably Informer used a Weather, WTH, which could be configured to use in a covariate setting. These models extract feature maps from the temporal dimension and extend the vanilla Transformer attention mechanism to produce more accurate predictions over longer forecast horizons in an autoregressive manner. A study by Zeng et al [12] found that the inclusion of covariates in transformer networks were largely ineffective, proposing instead simple linear models with seasonal decomposition similar to traditional state space ETS models.

Chen et al, proposed TSMixer [13], a FCC architecture which reshapes the inputs to force the network to learn across feature and temporal dimension in an attempt to improve multivariate performance.

3 Methodology

In this section, we outline our methodology for assessing the effectiveness of LSTM networks in multivariate time series prediction tasks, particularly focusing on the impact of time-dependent covariates.

3.1 Problem Statement

We consider a dataset containing M timeseries where each timeseries contains T historical observations, \mathbf{y} and covariates \mathbf{X} with k dimensions or individual features such that:

$$\mathbf{y} = [y_1, y_2, \dots, y_T]$$

$$\mathbf{X} = \begin{bmatrix} x_1^{(1)} & x_1^{(2)} & \dots & x_1^{(k)} \\ x_2^{(1)} & x_2^{(2)} & \dots & x_2^{(k)} \\ \vdots & \vdots & \ddots & \vdots \\ x_T^{(1)} & x_T^{(2)} & \dots & x_T^{(k)} \end{bmatrix}$$

Let $\mathbf{Z} = \mathbf{y} \oplus \mathbf{X}$. The objective of the training task is to forecast a vector of future values and covariates across a forecast horizon H . At each timestep t , this vector is represented as $\hat{\mathbf{z}}_t = [\hat{y}_t, \hat{x}_t^1, \hat{x}_t^2, \dots, \hat{x}_t^k]$ where \hat{y}_t is the predicted target variable and $\hat{x}_t^1, \hat{x}_t^2, \dots, \hat{x}_t^k$ are the predicted future covariates.

During model evaluation, we derive the vector of predicted target variables, $\hat{\mathbf{y}}$ from $\hat{\mathbf{Z}}$ such that $\hat{\mathbf{y}} = [\hat{y}_1, \hat{y}_2, \dots, \hat{y}_H]$. The aim here is to generate $\hat{\mathbf{y}}$ in a manner that ensures it's more accurate than what could be achieved solely by relying on historical observations.

3.2 Datasets

We selected four publicly available datasets from the Monash repository [3] namely Hospital [14], Tourism [15], Traffic [16] and Electricity [17]. These datasets are from diverse domains and have been extensively benchmarked in prior research by Godahewa et al [3] and are commonly used for evaluating time series forecasting models. The Hospital dataset consists of 767 monthly time series depicting patient counts related to medical products from January 2000 to December 2006. Similarly, the Electricity dataset was used by Lai [6] and represents the hourly electricity consumption of 321 clients from 2012 to 2014. The Tourism dataset comprises monthly figures from 1311 tourism-related time series, while the Traffic dataset includes 862 weekly time series showing road occupancy rates on San Francisco Bay area freeways from 2015 to 2016. Each dataset is accompanied by specific context lengths C (lookback window) and forecast horizons H , providing a robust evaluation framework.

3.3 Covariate Data Augmentation

Since the original datasets do not contain time-dependent covariates, we artificially augment them to introduce covariates correlated with future target values such that x_t^k is correlated with y_{t+k} . When $k=3$, for example, the network is supplied with 3 covariates correlated with the following 3 target values. The network would have to learn that the value of the covariate, x_t^k , would take effect on target, y , at a time k timesteps in the future.

Noise is added to each leading indicator to control the level of cross correlation between the covariate and its corresponding target. The noise is calculated as follows:

- For each time series in the dataset the mean μ and standard deviation σ of y are computed.
- For each covariate value a sample ϵ is drawn from a unit normal distribution; $\epsilon \sim N(0, 1)$
- The noise is computed by scaling the random ϵ values by μ and σ and then further scaled by an error level factor γ : $\gamma \in \{0, 0.1, \dots, 1.9\}$

Let $\mathbf{x}^{(k)}$ be the augmented covariate input sequence $[x_0, x_1, \dots, x_T]$, then $x_t^k = y_{t+k} + \gamma \cdot \mu \cdot \epsilon + \gamma \cdot \sigma \cdot \epsilon$. We then compute the cross correlation between the covariates and the target variables with the Pearson

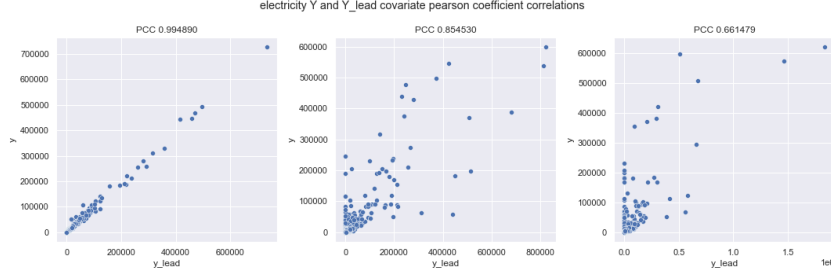


Figure 1: Plots of various correlations between covariate and target variables on the Electricity dataset

correlation coefficient (*PCC*) and aim for each experiment to be run with a strong to perfect positive correlation in the range 0.5 to 1.0. This value is then directly comparable to autocorrelation of lagged variables used in techniques such as ARIMA as described by Hyndman et al [18].

3.4 Model architectures

To better understand how covariates affect our results and attribute their impact more accurately, we employed two straightforward LSTM based architectures. Unlike the deep learning models benchmarked by Monash [3] which used the GluonTS [19] framework for training, we did not add covariates such as lag variables and static time-series identifiers in order to accurately evaluate the true effect of the augmented leading covariates.

Of these models: base-lstm is used as a baseline and is benchmarked against the Monash repository results using the same context length C and forecast horizons H ; while the seg-lstm model is intended to be more capable of forecasting over longer horizons using longer context lengths.

3.4.1 Baseline model (base-lstm)

Baseline is a vanilla LSTM with a scaling strategy inspired by DeepAR[1]. The input data is scaled using mean absolute scaling within each mini-batch. An additional time dependent feature $\log(scale)$ is concatenated with the input vector. The scaled values are fed into a 2 layer LSTM with 40 cells in each layer. The output of the LSTM is then fed into a single fully connected layer with 40 cells followed by ReLU activations. Finally, an output layer generates a vector \mathbf{z}_t containing the predicted target variable \hat{y}_t and predicted covariates $\hat{\mathbf{x}}_t$. An inverse scaling operation finally transforms the predictions back into the original scale.

3.4.2 Segment model (seg-lstm)

The seg-lstm model addresses the limitation of the baseline model in forecasting over longer time horizons. Our approach aims to maximise historical data without relying on extra features, such as lag variables that get applied with GluonTS [19] models and is typical with transformer based approaches [9, 10, 11, 8].

To achieve this, we propose an LSTM with a simple modification to handle input data. We reshape each context window of C values into a vector of dimension $\frac{C}{d} \times d$, where d represents the segment length, typically set to the seasonality of the data (e.g., 24 for hourly readings).

The model architecture is similar to the base-lstm, consisting of a straightforward LSTM with 2 layers and 40 cells in each layer, followed by fully connected layers with ReLU activations. We use mean absolute scaling but omit the additional time-dependent feature $\log(scale)$.

During training, we compute the loss by comparing the last timestep of each segment output to the corresponding timestep in the target vector shifted one step into the future. The network is trained to predict one timestep ahead from each segment, with hidden state representations derived from segments are separated by a time period d .

During inference, we predict the next timestep vector, append it to the previous timestep segment, and drop the oldest vector \mathbf{z}_{t_0} . This forms an autoregressive loop, predicting successive segments of adjacent timesteps rather than spanning a fixed time period d .

3.5 Evaluation Metrics

We evaluate the performance of each model using MAE, RMSE, and sMAPE, computed on the raw (i.e. unscaled) values of the dataset. This approach ensures direct comparability with results from the Monash archive[3], enabling comprehensive assessment and comparison.

$$\begin{aligned} \text{MAE}(\hat{Y}, Y) &= \frac{\sum_{t=1}^H |\hat{Y}_t - Y_t|}{H} & \text{RMSE}(\hat{Y}, Y) &= \sqrt{\frac{\sum_{t=1}^H (\hat{Y}_t - Y_t)^2}{H}} \\ \text{sMAPE}(\hat{Y}, Y) &= \frac{100\%}{H} \sum_{t=1}^H \frac{|\hat{Y}_t - Y_t|}{(|\hat{Y}_t| + |Y_t|)/2} \end{aligned}$$

4 Experimental Setup

We now describe the details of the experiments including how the data was processed, the model training and evaluation.

4.1 Data Processing

To facilitate model training, we generate time windows of data, each of which is equal in size to the sum of the context length (C) and the forecast horizon (H). During each training epoch, complete and overlapping windows are extracted from each time series.

The dataset is partitioned into training, validation, and test sets, following a chronological order. The validation set excludes values within the last forecast horizon, while the training set excludes values from the last two forecast horizons. Evaluation for both validation and testing is conducted on the last complete forecast horizon period of each time series. This approach ensures direct comparison to the Monash benchmarks [3] and maximises the utilisation of training data while preventing data leakage between the three sets.

We employ a variation of mean absolute scaling to standardise the data within each mini-batch (local normalisation), accounting for batches with values equal to zero.

$$\text{scale}(\mathbf{z}) = \max\left(\frac{\sum_{t=1}^C |z_t^{(y)}|}{C}, 1\right) \quad (1)$$

4.2 Training

We utilised teacher forcing which trains the network to predict a single timestep ahead and calculated the loss for the entire sequence (ie the context length and the forecast horizon). The network was trained as a regression task with a Smooth F1 Loss objective.

$$\text{SmoothL1Loss}(\hat{z}, z) = \begin{cases} 0.5(\hat{z} - z)^2 & \text{if } |\hat{z} - z| < 1 \\ |\hat{z} - z| - 0.5 & \text{otherwise} \end{cases} \quad (2)$$

A number of hyperparameters were set to match the default GluonTS parameters [19] including weight decay of $1e-8$; dropout of 0.1; and a learning rate of 0.001. We used OneCycle scheduling to anneal and then decrease the learning rate[20] over 100 epochs. The models were optimised using AdamW. We made no attempt to optimise hyperparameters.

Performance was measured on the validation set at the end of each epoch by measuring the Smooth L1 loss using free running (i.e. using the predicted outputs of one timestep as the input into the next). The model checkpoint with the lowest validation loss was selected for testing. The hidden state of the LSTM was initialised to 0.

Table 1: Benchmark results for each dataset

Models		FFNN	DeepAR	N-Beats	Wavenet	Transformer	base-lstm*	seg-lstm*
Hospital (12)	sMAPE	18.33	17.45	17.77	17.55	20.08	17.52	18.05
	MAE	22.86	18.25	20.18	19.35	36.19	18.03	19.95
	RMSE	27.77	22.01	24.18	23.38	40.48	22.03	24.19
Tourism (24)	sMAPE	20.11	18.35	20.42	18.92	19.75	21.50	19.85
	MAE	2022.21	1871.69	2003.02	2095.13	2146.98	2336.42	1956.07
	RMSE	2584.10	2359.87	2596.21	2694.22	2660.06	2964.96	2413.64
Traffic (8)	sMAPE	12.73	13.22	12.40	13.30	15.28	12.77	12.97
	MAE	1.15	1.18	1.11	1.20	1.42	1.15	1.17
	RMSE	1.55	1.51	1.44	1.61	1.94	1.56	1.58
Electricity (168)	sMAPE	23.06	20.96	23.39	-	24.18	34.12	21.20
	MAE	354.39	329.75	350.37	286.56	398.80	525.50	287.95
	RMSE	519.06	477.99	510.91	489.91	514.68	675.03	469.07

* Mean values from 5 runs.

Forecast horizons are given in the brackets

4.3 Experimental Procedure

Initially, we trained base-lstm models for each dataset using the context length and forecast horizon values consistent with those used in the Monash repository which allowed us to compare the performance of our models against benchmarked results.

Next, we trained and evaluated models under various scenarios involving 1, 2 and 3 covariates. For the number of covariates in the scenario a set of base-lstm models were trained with increased noise to vary the level of cross correlation with the target variables. This allows us to assess the impact of covariates on model performance under different correlation levels. These models were trained to a context length and forecast horizon that equalled the benchmarked results from Monash [3]

We then trained seg-lstm models using the same procedure with the exception that we use a longer context length C which was set to 3x the forecast horizon H on Hospital, Tourism and Electricity and 8x the forecast horizon on Traffic.

5 Results

Table 1 presents the mean error metrics for each dataset evaluated against the neural network architectures benchmarked by Godahewa et al [3]. Among these architectures, FFNN and N-BEATS [21] are fully-connected models, while DeepAR [1] is based on an LSTM network. WaveNet [22], originally designed for audio synthesis, was adapted by Alexandrov et al [19] for time-series tasks in GluonTS. Additionally, the Transformer architecture closely follows the implementation described in the original paper by Vaswani et al [23].

Comparing the base-lstm model across datasets, it yielded comparable results on the Hospital and Traffic datasets, slightly inferior results on Tourism, and significantly poorer results on Electricity when measured by sMAPE. However, the performance is marginally better when evaluated using MAE and RMSE. Notably, the base-lstm model exhibited relatively better performance on datasets with shorter forecast horizons.

The seg-lstm model emerged as the top performer on Electricity with RMSE and second with MAE and sMAPE, whilst on Tourism it ranked second with MAE and RMSE, both of which have longer forecast horizons. Overall, both of our models demonstrated comparable performance to the benchmarks on the shorter forecast horizons of Hospital and Traffic, while the seg-lstm model also displayed competitive performance on Tourism and Electricity.

Table 2: sMAPE results for covariates $k \in \{0, 1, 2, 3\}$ and cross correlation $PCC \in \{1, 0.9, 0.5\}$

Models		base-lstm			seg-lstm		
<i>PCC</i>		1	0.9	0.5	1	0.9	0.5
Hospital (12)	k=0	17.52 \pm 0.041	17.52 \pm 0.041	17.52 \pm 0.041	18.05 \pm 0.135	18.05 \pm 0.135	18.05 \pm 0.135
	k=1	16.13	17.45	17.77	16.07	17.96	18.09
	k=2	14.94	17.65	18.06	17.33	18.49	18.51
	k=3	13.49	17.71	17.72	17.71	17.68	18.77
Tourism (24)	k=0	21.50 \pm 0.531	21.50 \pm 0.531	21.50 \pm 0.531	19.85 \pm 0.62	19.85 \pm 0.62	19.85 \pm 0.62
	k=1	20.54	22.17	28.18	19.14	20.32	21.56
	k=2	20.26	24.33	27.64	19.07	20.49	21.84
	k=3	23.08	27.59	28.13	18.61	19.96	23.06
Traffic (8)	k=0	12.77 \pm 0.065	12.77 \pm 0.065	12.77 \pm 0.065	12.97 \pm 0.108	12.97 \pm 0.108	12.97 \pm 0.108
	k=1	11.36	12.59	12.89	11.64	12.85	13.00
	k=2	10.73	12.15	12.62	11.10	13.12	12.86
	k=3	9.57	11.86	13.51	9.88	11.94	12.90
Electricity (168)	k=0	34.12 \pm 2.38	34.12 \pm 2.38	34.12 \pm 2.38	21.20 \pm 0.232	21.20 \pm 0.232	21.20 \pm 0.232
	k=1	33.10	30.41	33.95	21.01	22.37	21.45
	k=2	33.62	30.42	38.16	21.14	22.48	22.11
	k=3	36.18	33.83	31.50	21.61	23.04	22.20

Forecast horizons given in the brackets. Univariate k=0 intervals are 95% CI.

5.1 Covariates

The results of covariates compared to univariate cases are presented in table 2. For brevity we have included *PCC* values of 1, 0.9 and 0.5 (See appendix for details of complete results) and show the sMAPE for each dataset at the full forecast horizons as measured in the benchmark tests. We present the results for each value of k covariates tested (1, 2 and 3) and compare it to the univariate case where $k=0$. To some extent the relative differences between the covariate and univariate cases are somewhat specific to the dataset. The models trained on *Traffic* appear to benefit the most from covariates giving improved results in 14 of the 18 experiments, which is perhaps to be expected as this has the shortest forecast horizon. Conversely models performed worst on, *Tourism* only outperforming univariate in 5 scenarios, and that was with perfectly correlated covariates. *Electricity*, which has the longest forecast horizon of 168, marginally outperformed univariate in both models with $PCC = 1.0$ using 1 and 2 covariates.

5.1.1 Comparing PCC at forecast horizons = k

We are interested in analysing the performance of models in the special cases where the forecast horizon matches the number of covariates, as in these cases the model is effectively provided with information required to predict each timestep. Specifically, we wanted to understand the role that the cross correlation plays on model performance. Figure 2 shows how the base-lstm model sMAPE degrades as a function of *PCC* on each of the datasets where the forecast horizon is 3. Models with 1 and 2 covariates exhibit similar traits, see Appendix. Unsurprisingly the performance is best when the correlation is perfect (ie $PCC = 1.0$) to the extent that an almost perfect prediction was obtained in the cases of *Traffic* and *Hospital*. However the performance degrades as the *PCC* decreases in a non linear manner, with the error increasing rapidly as the *PCC* falls to 0.9. Interestingly even in this highly artificial and advantageous setting, the error on *Tourism* and *Electricity* are still worse than the univariate case at correlation levels less than 0.9.

5.1.2 Comparing PCC over longer forecast horizon trajectories

With the exception of *Traffic*, as the forecast horizon extends any performance advantage over a univariate setting diminishes for a *PCC* value of 0.9 and below when forecast horizon exceeds 3-4 timesteps. Figure 3 plots the base-lstm sMAPE as a function of forecast horizon on the *Tourism* dataset.

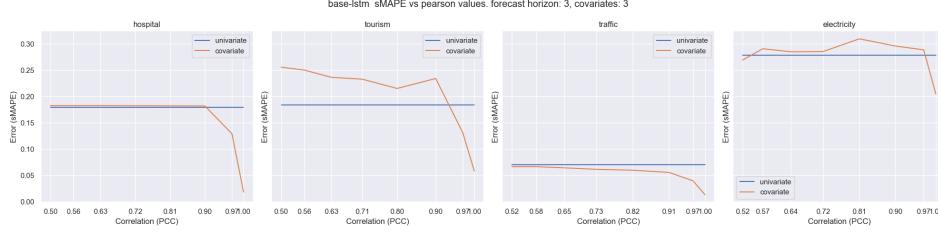


Figure 2: base-1stm smape as a function of PCC for 3 covariates

5.1.3 Comparing base-1stm and seg-1stm performance

Looking at the differences between base-1stm and seg-1stm. We see that both models share common characteristics when examining the errors on forecast horizon trajectories. The stronger model in univariate scenarios will also perform better in a covariate setting. Figure 3 shows how the sMAPE accumulates over the full forecast horizon on the Tourism dataset for both base-1stm and seg-1stm. Note how the variance of errors is smaller across the range of PCC values on the stronger seg-1stm model, indicating that the additional noise added to lower PCC covariates combines with the model's inherent performance limitations to compound errors over time.

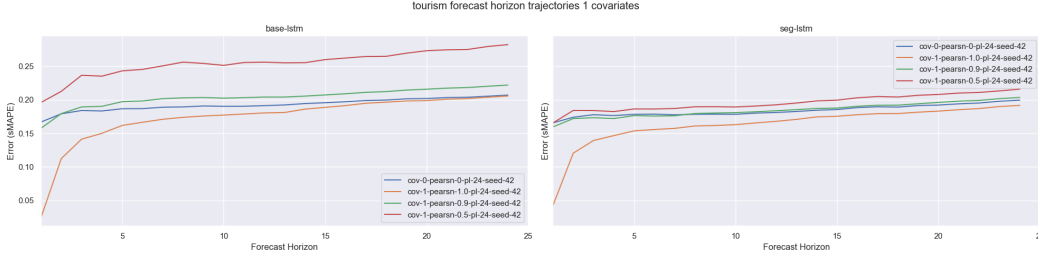


Figure 3: Tourism smape for 1 covariate for base-1stm and seg-1stm

5.1.4 Comparing covariates across Forecast Horizon trajectories

Turning to comparing multiple covariates. Fig 4 shows sMAPE across full forecast horizons for 1, 2 and 3 covariates on the Traffic dataset with the special case of perfect correlation ($PCC = 1$). Note that the error reduces as the number of covariates increases. Interestingly, the addition of each covariate shifts the onset of significant errors by one timestep. (i.e. errors start to accumulate at $t=1$ for $k=1$, at $t=2$ for $k=2$ and $t=3$ for $k=3$). We observe identical patterns on the other datasets tested. Clearly the network is effectively utilising the covariates to learn the values for the first k

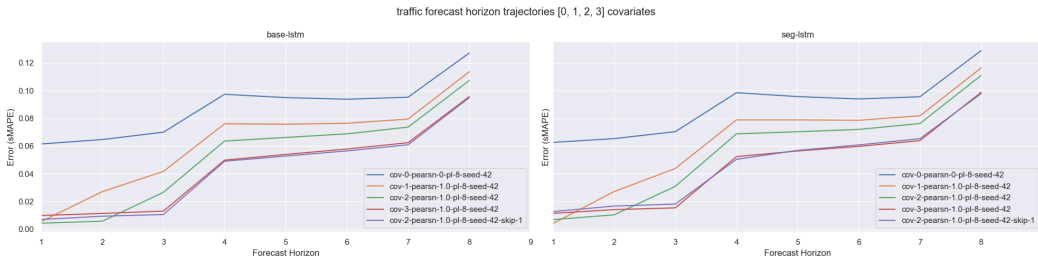


Figure 4: Traffic smape comparing univariate to 1, 2 and 3 covariates for base-1stm at $PCC = 0.9$

timesteps, however it is conceivable that a model may be using covariate values from the current timestep alone rather than utilising covariates from previous timesteps. For example in the case of 3 covariates x_t^1, x_t^2, x_t^3 are leading indicators for target values y_t, y_{t+1}, y_{t+2} , and therefore the network

does not require covariates from previous timesteps in order to predict the subsequent 3 timesteps to produce the error improvement that we observe. Consequently we don't know if the model is utilising covariates across the temporal dimension or if it is just using the current timestep's covariates.

One way to help answer this is to omit the x_t^2 covariate meaning that at any given timestep the input vector contains lead indicators for y_t and y_{t+2} and the model would have to obtain the leading covariate for y_{t+1} from x_{t-1}^3 (ie the previous timestep). If the error trajectory in this example continues to exhibit the same 3 timestep offset that we observe with 3 covariates then we reason that the model must be learning across both temporal and feature dimensions simultaneously. Figure 4 illustrates the comparison between the univariate and covariate cases. It is evident from the plotted series, labelled as *cov-2-pearsn-1.0-pl-8-seed-42-skip-1*, that the error closely resembles that of using 3 covariates.

6 Discussion

We have presented a repeatable method for testing the effectiveness of predicting covariates in neural networks that could be employed for alternative model architectures. Furthermore we have developed an LSTM model (seg-lstm) capable of producing state of the art results in a univariate setting on long forecast horizons without necessitating the need for additional features.

Analysis of results has led us to reach the following conclusions:

- An LSTM is able to model both temporal and feature dynamics at short forecast horizons in the presence of short lead timestep covariates.
- The effect covariates have on performance is, in part, related to the characteristics of the task (dataset) that the model is trained on.
- The magnitude of the performance gain is related to the strength of the correlation between the covariate and the target variables and that this relationship is nonlinear with performance degrading most rapidly for *PCC* levels between 1.0 and 0.9.
- In most cases the presence of predicted covariates becomes either ineffective or a hindrance to performance as forecast horizons extend.
- The number of timesteps covered by multiple covariates can offset the accumulation of error equal to the number of timesteps.
- The magnitude of the performance advantage from using covariates is related to the model's underlying ability to forecast accurately. Models that perform better in a univariate setting will produce comparatively better results in a covariate setting.
- Increasing the number of covariates can enhance performance on short forecast horizons with the magnitude of the performance being related to the *PCC*

Given the aim of this study was to explore the effect of covariates on LSTM networks, it's evident that predicting covariates jointly with target variables can under very limited conditions result in a performance improvement. As forecast horizons extend however, it frequently hinders performance. While acknowledging the artificial nature of the experiments used in this study it nonetheless underscores some potential for covariates to assist neural networks in making more accurate predictions.

It may be possible that the vanilla LSTM's struggle to learn the relationships between covariates and target variables across long forecast horizons and that alternative architectures and/or additional feature engineering techniques (such as LSTNet [6] and the transformer based models of Zhou, Kitaeo and Zhang [9, 8, 11]) may perform better and a future study could evaluate their effectiveness using the same conditions.

Future studies could also evaluate the use of covariates with more representative real-world data, such as the work by Zhou [9] using the weather dataset which contains multiple features related to predicting weather. Additionally, further exploration with artificial datasets could investigate the effects of other characteristics like extending the covariate lead time offset on target variables, non-stationarity or negative correlations. This raises the question of whether providing the network with information regarding the temporal influence of each leading indicator on the target variable could simplify the learning task.

References

- [1] David Salinas, Valentin Flunkert, and Jan Gasthaus. Deepar: Probabilistic forecasting with autoregressive recurrent networks, 2019.
- [2] Jeffrey L. Elman. Finding structure in time. *Cognitive Science*, 14(2):179–211, 1990. doi: https://doi.org/10.1207/s15516709cog1402_1. URL https://onlinelibrary.wiley.com/doi/abs/10.1207/s15516709cog1402_1.
- [3] Rakshitha Godahewa, Christoph Bergmeir, Geoffrey I. Webb, Rob J. Hyndman, and Pablo Montero-Manso. Monash time series forecasting archive. In *NeurIPS Datasets and Benchmarks*. Curran Associates, Inc., 2021. URL <https://datasets-benchmarks-proceedings.neurips.cc/paper/2021/hash/eddea82ad2755b24c4e168c5fc2ebd40-Abstract-round2.html>.
- [4] Shuchun Wang. Exponential smoothing for forecasting and bayesian validation of computer models, 01 2006.
- [5] AC Puindi and ME Silva. Dynamic structural models with covariates for short-term forecasting of time series with complex seasonal patterns. *J Appl Stat*, 48(5):804–826, 2020. doi: 10.1080/02664763.2020.1748178.
- [6] Guokun Lai, Wei-Cheng Chang, Yiming Yang, and Hanxiao Liu. Modeling long- and short-term temporal patterns with deep neural networks, 2018.
- [7] David Salinas, Michael Bohlke-Schneider, Laurent Callot, Roberto Medico, and Jan Gasthaus. High-dimensional multivariate forecasting with low-rank gaussian copula processes, 2019.
- [8] Nikita Kitaev, Łukasz Kaiser, and Anselm Levskaya. Reformer: The efficient transformer, 2020.
- [9] Haoyi Zhou, Shanghang Zhang, Jieqi Peng, Shuai Zhang, Jianxin Li, Hui Xiong, and Wancai Zhang. Informer: Beyond efficient transformer for long sequence time-series forecasting, 2021.
- [10] Haixu Wu, Jiehui Xu, Jianmin Wang, and Mingsheng Long. Autoformer: Decomposition transformers with auto-correlation for long-term series forecasting, 2022.
- [11] Yunhao Zhang and Junchi Yan. Crossformer: Transformer utilizing cross-dimension dependency for multivariate time series forecasting. In *The Eleventh International Conference on Learning Representations*, 2023. URL <https://openreview.net/forum?id=vSVLM2j9eie>.
- [12] Ailing Zeng, Muxi Chen, Lei Zhang, and Qiang Xu. Are transformers effective for time series forecasting?, 2022.
- [13] Si-An Chen, Chun-Liang Li, Nate Yoder, Sercan O. Arik, and Tomas Pfister. Tsmixer: An all-mlp architecture for time series forecasting, 2023.
- [14] Rakshitha Godahewa, Christoph Bergmeir, Geoff Webb, Rob Hyndman, and Pablo Montero-Manso. Hospital dataset, apr 2021. URL <https://doi.org/10.5281/zenodo.4656014>.
- [15] Rakshitha Godahewa, Christoph Bergmeir, Geoff Webb, Rob Hyndman, and Pablo Montero-Manso. Tourism monthly dataset, apr 2021. URL <https://doi.org/10.5281/zenodo.4656096>.
- [16] Rakshitha Godahewa, Christoph Bergmeir, Geoff Webb, Rob Hyndman, and Pablo Montero-Manso. Traffic weekly dataset, apr 2021. URL <https://doi.org/10.5281/zenodo.4656135>.
- [17] Rakshitha Godahewa, Christoph Bergmeir, Geoff Webb, Rob Hyndman, and Pablo Montero-Manso. Electricity hourly dataset, apr 2021. URL <https://doi.org/10.5281/zenodo.4656140>.
- [18] R.J. Hyndman and G. Athanasopoulos. *Forecasting: principles and practice*. OTexts, Melbourne, Australia, 3 edition, 2021. URL <https://OTexts.com/fpp3>. Accessed on 2024-03-21.

- [19] A. Alexandrov, K. Benidis, M. Bohlke-Schneider, V. Flunkert, J. Gasthaus, T. Januschowski, D. C. Maddix, S. Rangapuram, D. Salinas, J. Schulz, L. Stella, A. C. Türkmen, and Y. Wang. GluonTS: Probabilistic Time Series Modeling in Python. *arXiv preprint arXiv:1906.05264*, 2019.
- [20] Leslie N. Smith and Nicholay Topin. Super-convergence: Very fast training of neural networks using large learning rates, 2018.
- [21] Boris N. Oreshkin, Dmitri Carpov, Nicolas Chapados, and Yoshua Bengio. N-beats: Neural basis expansion analysis for interpretable time series forecasting, 2020.
- [22] Aaron van den Oord, Sander Dieleman, Heiga Zen, Karen Simonyan, Oriol Vinyals, Alex Graves, Nal Kalchbrenner, Andrew Senior, and Koray Kavukcuoglu. Wavenet: A generative model for raw audio, 2016.
- [23] Ashish Vaswani, Noam Shazeer, Niki Parmar, Jakob Uszkoreit, Llion Jones, Aidan N. Gomez, Lukasz Kaiser, and Illia Polosukhin. Attention is all you need, 2023.

A Appendix / supplemental material

A.1 Datasets

All datasets used in this study are available through the Monash repository <https://forecastingdata.org/> and are distributed under a Creative Commons Attribution 4.0 International licence.

A.2 hyperparameters

Table 3: hyperparameters

learning rate	0.001
epochs	100
hidden cells	40
lstm hidden layers	2
dropout	0.1
weight decay	1e-8
batch size	128
batches per epoch	200 (base-lstm) 500 (seg-lstm)
early stopping patience	30
optimizer	AdamW
scheduler	OneCycle

A.3 Computational Details

All models were trained using CPU.
memory: 18 GB
os: macOS-10.16-x86_64-i386-64bit
python 3.11

A.4 Source Code

The models were developed using Pytorch. Source code is available at <https://github.com/garethmd/nnts/tree/rnn-covariates-paper>

Table 4: total model training times

Dataset	Model	
	base-lstm (seconds)	seg-lstm (seconds)
Electricity	70442	51839
Hospital	11029	1151
Tourism	20412	6807
Traffic	15667	2652

* Each dataset is trained with 30 models.

A.5 Additional Results

CSV Files of the full results are available on Google Drive

<https://drive.google.com/drive/folders/179UK0lOOSi7yRdXOhcd7AFKl9U9A1DpE?usp=sharing> In this section we present additional tables and plots of results which supplement the results in the main paper.

Table 5 details the MAE error for the base-lstm model for each dataset with various k covariates and correlation PCC values.

Table 6 details the MAE error for the seg-lstm model for each dataset with various k covariates and correlation PCC values.

Table 7 details the RMSE error for the base-lstm model for each dataset with various k covariates and correlation PCC values.

Table 8 details the RMSE error for the seg-lstm model for each dataset with various k covariates and correlation PCC values.

Table 5: MAE base-lstm results for covariates $k \in \{0, 1, 2, 3\}$ and cross correlation $PCC \in \{1, 0.9, 0.5\}$ values.

Models		base-lstm		
PCC		1	0.9	0.5
Hospital (12)	k=0	18.03 \pm 0.306	18.03 \pm 0.306	18.03 \pm 0.306
	k=1	16.71	19.03	20.18
	k=2	15.62	20.31	20.77
	k=3	14.49	20.18	20.23
Tourism (24)	k=0	2336.42 \pm 147.6	2336.42 \pm 147.6	2336.42 \pm 147.6
	k=1	2131.98	2545.43	3437.56
	k=2	2352.32	3734.32	4014.21
	k=3	3593.42	3340.92	3574.85
Traffic (8)	k=0	1.15 \pm 0.010	1.15 \pm 0.010	1.15 \pm 0.010
	k=1	1.03	1.14	1.16
	k=2	0.95	1.09	1.14
	k=3	0.84	1.06	1.23
Electricity (168)	k=0	525.50 \pm 51.74	525.50 \pm 51.74	525.50 \pm 51.74
	k=1	505.01	526.33	596.59
	k=2	528.35	452.38	519.68
	k=3	631.98	510.47	525.58

Forecast horizons given in the brackets. Univariate k=0 intervals are 95% CI.

Table 6: MAE seg-lstm results for covariates $k \in \{0, 1, 2, 3\}$ and cross correlation $PCC \in \{1, 0.9, 0.5\}$ values.

Models		seg-lstm		
PCC		1	0.9	0.5
Hospital (12)	k=0	19.95 \pm 0.309	19.95 \pm 0.309	19.95 \pm 0.309
	k=1	16.73	20.83	21.55
	k=2	20.05	23.14	23.46
	k=3	21.34	22.22	24.93
Tourism (24)	k=0	1956.07 \pm 163.4	1956.07 \pm 163.4	1956.07 \pm 163.4
	k=1	2078.31	3180.39	2292.99
	k=2	1782.48	3176.35	2857.37
	k=3	2053.37	2136.06	2790.61
Traffic (8)	k=0	1.17 \pm 0.021	1.17 \pm 0.021	1.17 \pm 0.021
	k=1	1.04	1.16	1.17
	k=2	0.98	1.19	1.15
	k=3	0.87	1.07	1.16
Electricity (168)	k=0	287.95 \pm 50.88	287.95 \pm 50.88	287.95 \pm 50.88
	k=1	286.77	305.21	290.34
	k=2	288.11	306.79	297.81
	k=3	298.37	319.63	312.56

Forecast horizons given in the brackets. Univariate k=0 intervals are 95% CI.

Table 7: RMSE base-lstm results for covariates $k \in \{0, 1, 2, 3\}$ and cross correlation $PCC \in \{1, 0.9, 0.5\}$ values.

Models		base-lstm		
PCC		1	0.9	0.5
Hospital (12)	k=0	22.03 \pm 0.339	22.03 \pm 0.339	22.03 \pm 0.339
	k=1	20.95	23.22	24.53
	k=2	20.18	24.62	25.15
	k=3	19.65	24.51	24.55
Tourism (24)	k=0	2964.96 \pm 155.8	2964.96 \pm 155.8	2964.96 \pm 155.8
	k=1	2764.97	3178.28	4409.48
	k=2	3116.47	4706.51	5015.75
	k=3	4575.04	4361.75	4730.95
Traffic (8)	k=0	1.56 \pm 0.010	1.56 \pm 0.010	1.56 \pm 0.010
	k=1	1.47	1.55	1.58
	k=2	1.40	1.49	1.52
	k=3	1.28	1.46	1.68
Electricity (168)	k=0	675.03 \pm 5.865	675.03 \pm 5.865	675.03 \pm 5.865
	k=1	650.48	689.42	734.66
	k=2	680.63	606.75	666.07
	k=3	783.84	675.23	668.15

Forecast horizons given in the brackets. Univariate k=0 intervals are 95% CI.

Table 8: RMSE seg-lstm results for covariates $k \in \{0, 1, 2, 3\}$ and cross correlation $PCC \in \{1, 0.9, 0.5\}$ values.

Models		seg-lstm		
PCC		1	0.9	0.5
Hospital (12)	k=0	24.19 ± 0.434	24.19 ± 0.434	24.19 ± 0.434
	k=1	20.99	25.47	26.41
	k=2	24.55	27.93	28.27
	k=3	26.12	26.92	30.01
Tourism (24)	k=0	2964.96 ± 155.8	2964.96 ± 155.8	2964.96 ± 155.8
	k=1	2612.12	3803.94	2833.16
	k=2	2228.58	3875.71	3497.33
	k=3	2647.94	2660.67	3467.14
Traffic (8)	k=0	1.56 ± 0.010	1.56 ± 0.010	1.56 ± 0.010
	k=1	1.48	1.57	1.57
	k=2	1.44	1.61	1.55
	k=3	1.32	1.45	1.53
Electricity (168)	k=0	469.07 ± 7.734	469.07 ± 7.734	469.07 ± 7.734
	k=1	481.60	482.13	472.95
	k=2	474.75	488.84	473.14
	k=3	481.93	500.84	492.91

Forecast horizons given in the brackets. Univariate k=0 intervals are 95% CI.

Figures 5 plots the sMAPE as a function of correlation (PCC) for base-lstm models

Figures 6 plots the sMAPE as a function of correlation (PCC) for seg-lstm models

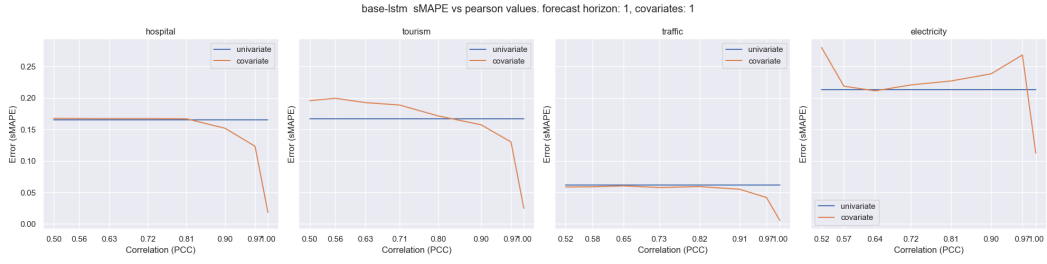
Figures 7 plots sMAPE for various covariates as a function of Forecast Horizon for correlation (PCC) = 1.0

Figures 8 plots sMAPE hospital forecast horizon trajectories for various covariates k and correlation values (PCC)

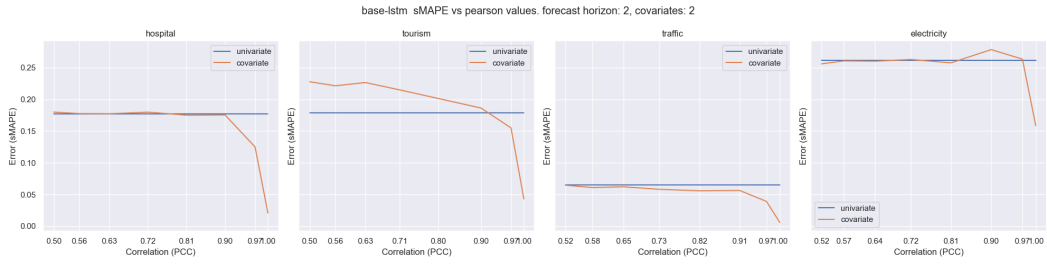
Figures 9 plots sMAPE tourism forecast horizon trajectories for various covariates k and correlation values (PCC)

Figures 10 plots sMAPE traffic forecast horizon trajectories for various covariates k and correlation values (PCC)

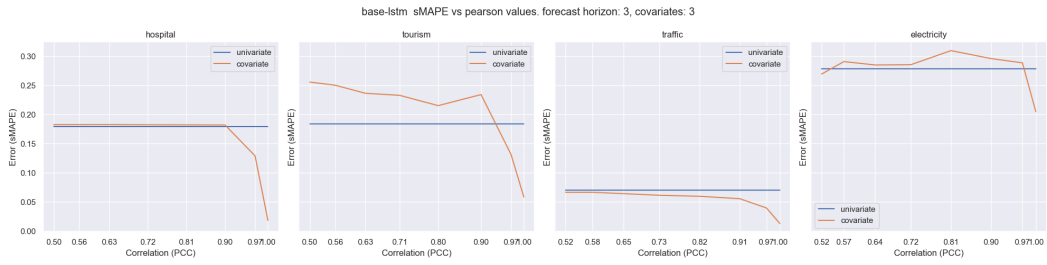
Figures 11 plots sMAPE electricity forecast horizon trajectories for various covariates k and correlation values (PCC)



(a) base- lstm sMAPE as a function of PCC for 1 covariate

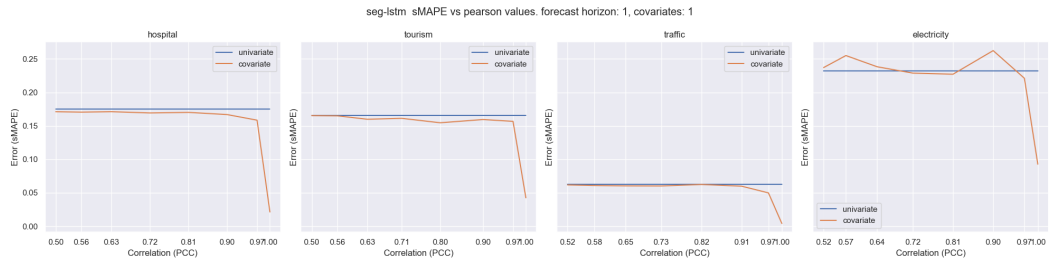


(b) base- lstm sMAPE as a function of PCC for 2 covariates

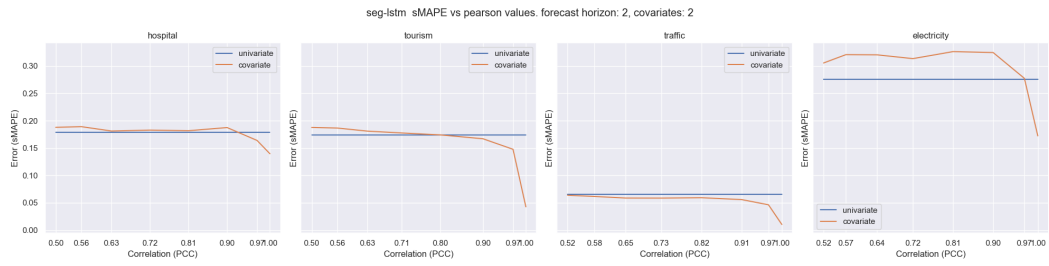


(c) base- lstm sMAPE as a function of PCC for 3 covariates

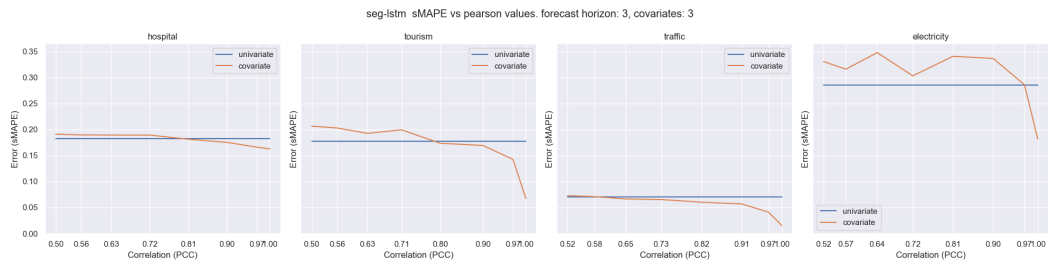
Figure 5: base- lstm sMAPE for various covariates as a function of correlation (PCC)



(a) seg-lstm sMAPE as a function of PCC for 1 covariate

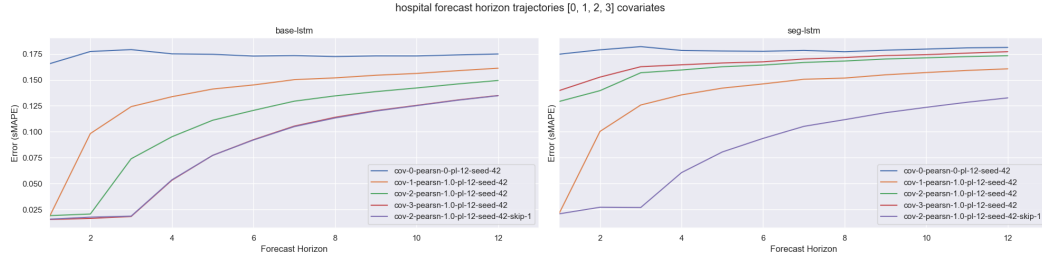


(b) seg-lstm sMAPE as a function of PCC for 2 covariates

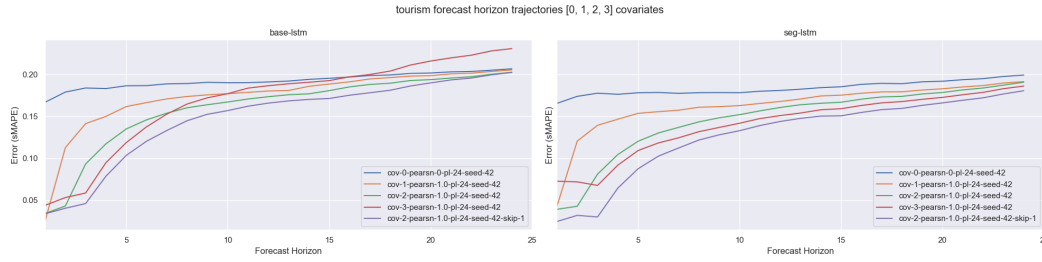


(c) seg-lstm sMAPE as a function of PCC for 3 covariates

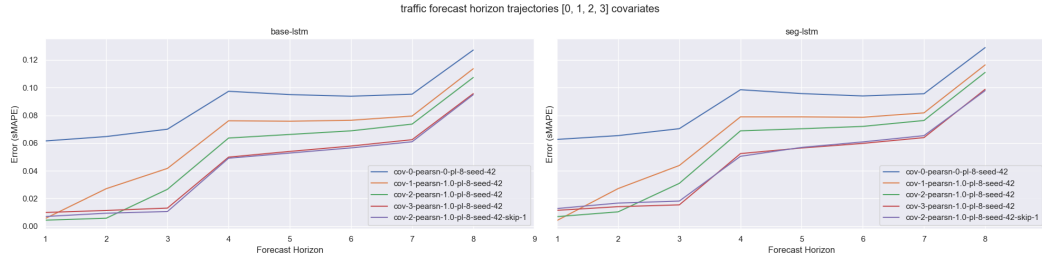
Figure 6: seg-lstm sMAPE for various covariates as a function of correlation (PCC)



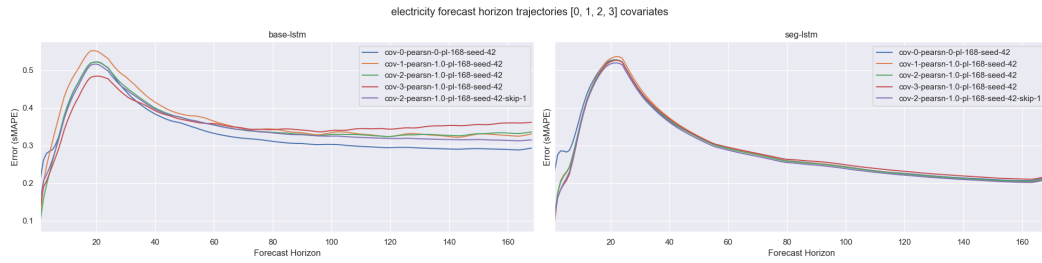
(a) hospital forecast horizon trajectories



(b) tourism forecast horizon trajectories

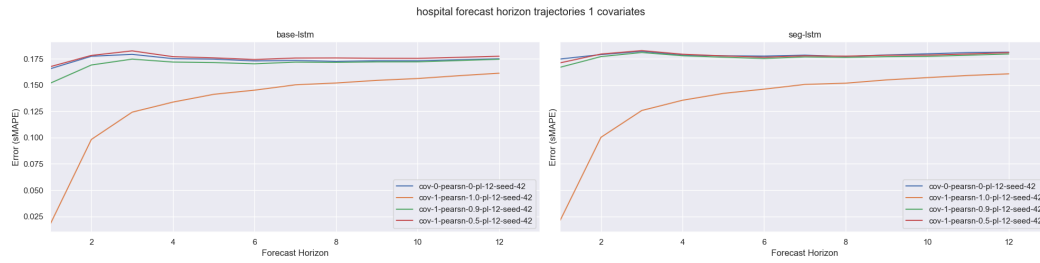


(c) traffic forecast horizon trajectories

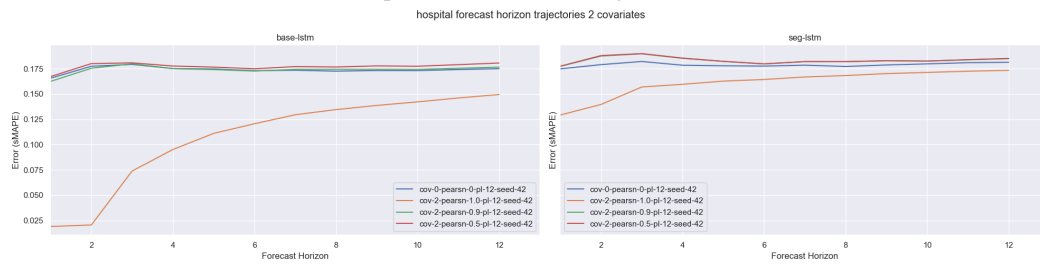


(d) electricity forecast horizon trajectories

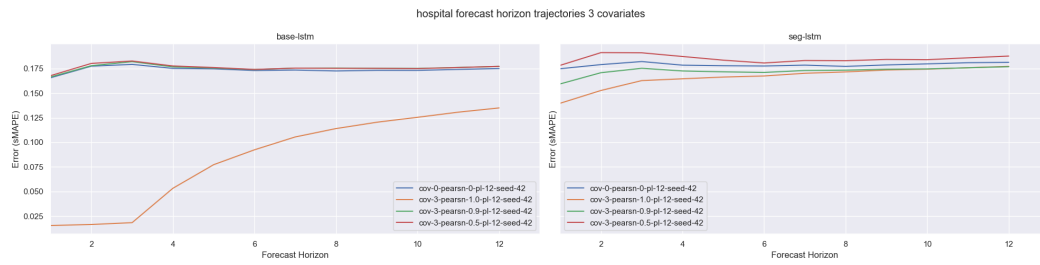
Figure 7: sMAPE for various covariates as a function of Forecast Horizon for correlation (PCC) = 1.0



(a) hospital forecast horizon trajectories k=1

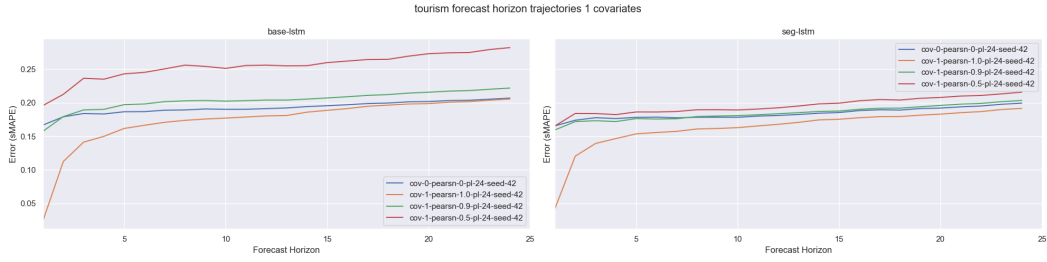


(b) hospital forecast horizon trajectories k=2

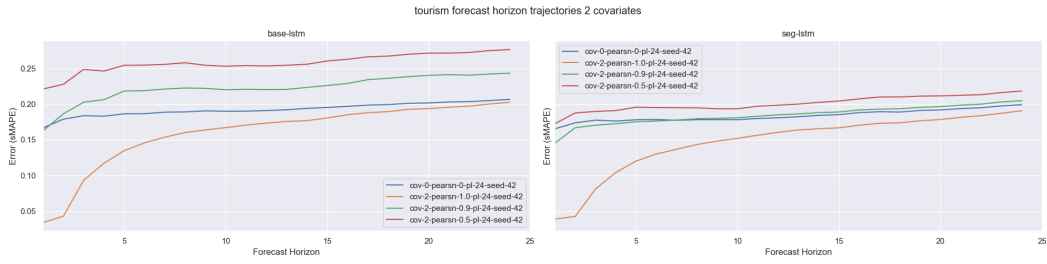


(c) hospital forecast horizon trajectories k=3

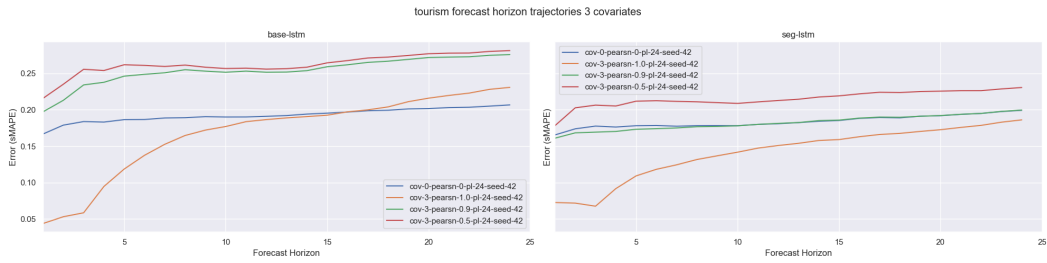
Figure 8: hospital forecast horizon trajectories for various covariates k and correlation values (PCC)



(a) tourism forecast horizon trajectories k=1

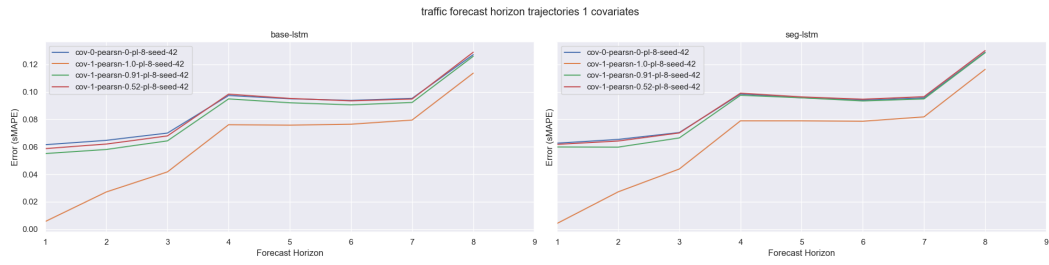


(b) tourism forecast horizon trajectories k=2

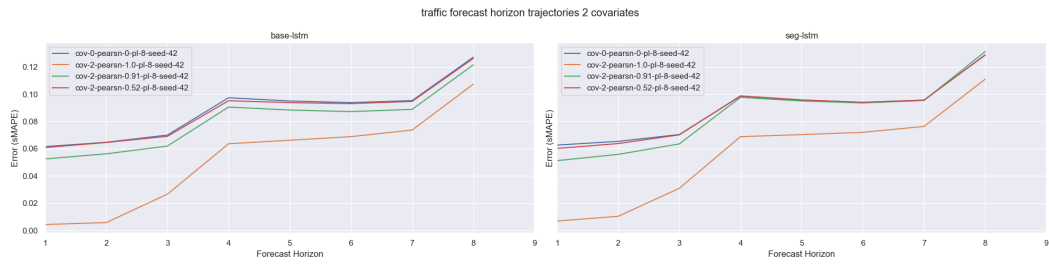


(c) tourism forecast horizon trajectories k=3

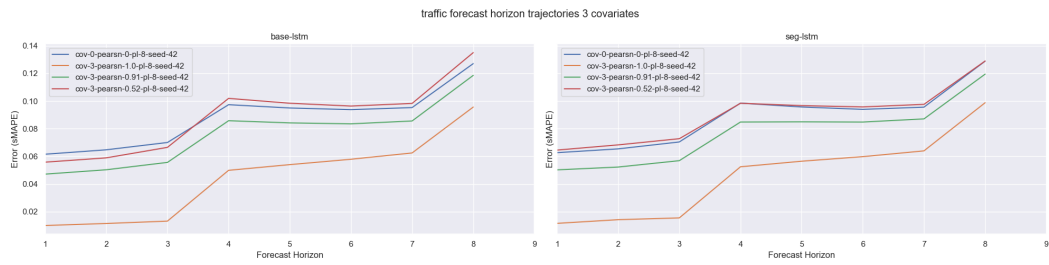
Figure 9: tourism forecast horizon trajectories for various covariates k and correlation values (PCC)



(a) traffic forecast horizon trajectories k=1

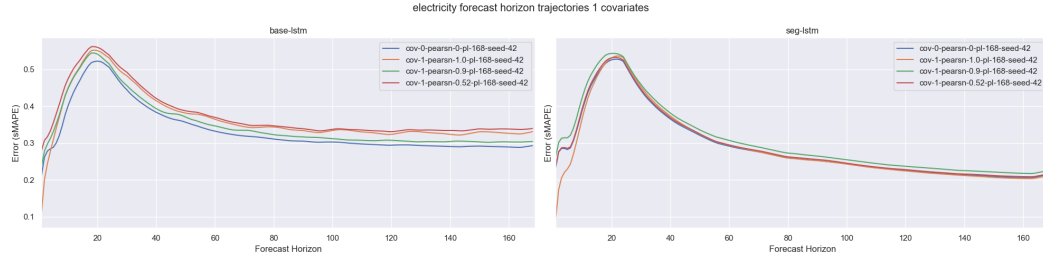


(b) traffic forecast horizon trajectories k=2

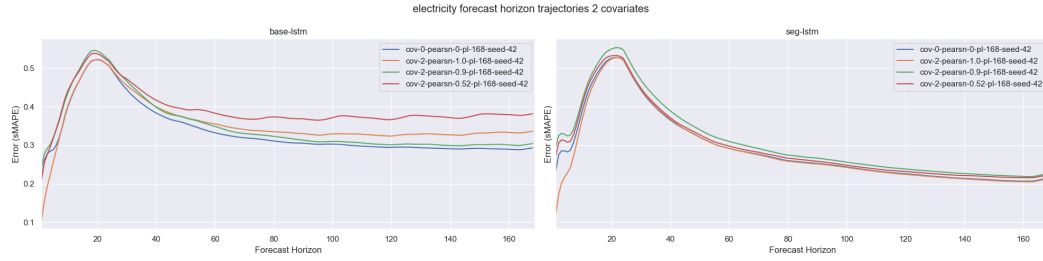


(c) traffic forecast horizon trajectories k=3

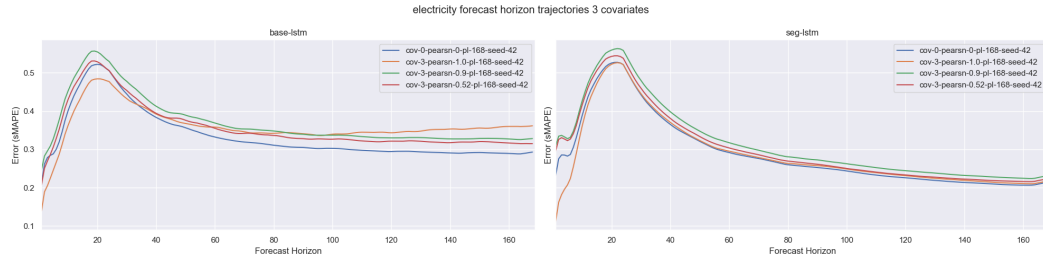
Figure 10: traffic forecast horizon trajectories for various covariates k and correlation values (PCC)



(a) electricity forecast horizon trajectories k=1



(b) electricity forecast horizon trajectories k=2



(c) electricity forecast horizon trajectories k=3

Figure 11: electricity forecast horizon trajectories for various covariates k and correlation values (PCC)